IPTC-11359-PP

Prediction of Thin Bed Reservoirs below ¼ Wavelength Tuning Thickness Using Full Bandwidth Inverted Seismic Impedance

Michael L. Shoemaker*, Jeff B. Robinson, Philip N. Trumbly, Bob A. Brennan, BP America, Inc.

This paper was prepared for presentation at the International Petroleum Technology Conference held in Dubai, U.A.E., 4–6 December 2007.

Abstract

Although conventional 3D reflection seismic data has been invaluable in the exploration and development of oil and gas fields worldwide, the stand-alone technology fundamentally lacks the resolution required to adequately characterize complex, thin-bedded hydrocarbon reservoirs. Limited vertical seismic resolution, implicitly defined at ¼ wavelength tuning thickness, can become particularly problematic when predicting reservoir dimensions, ultimately used for risk and reserve evaluation. Widess (1973) observed that thickness estimation of a "thin-bed", below ¼ wavelength tuning, can be detected (or is encoded) within the amplitude of the composite amplitude, which results from the increasing constructive interference of the top and base reflections as the bed thins. Herein, a methodology is introduced whereby aggregate reservoir sandstone thickness is successfully predicted away from well control via full bandwidth (0 to 25 Hz) inverted seismic impedance.

Thin bed reservoir thickness prediction utilizing inverted seismic impedance has been successfully applied in the onshore Tuscaloosa deep gas (7000 m) trend located in Louisiana, USA, where gross reservoir sandstones less then 40 meters thick are below ¼ tuning thickness. Well logs from 120 wells were used to regionally calibrate the 3D seismic cube to subsurface stratigraphy. A precise calibration allows for accurate rock property and seismic stratigraphic analysis, and tuning-wedge-type modeling; the results of which confirm that seismic amplitude response at Tuscaloosa is true to tuning phenomena, rather than rock property / fluid saturation effects. The 3D full bandwidth inverted seismic impedance data were linearly transformed to a sandstone thickness cube (in meters) well below ⅛ tuning thickness thus doubling seismic thickness prediction. This technique has resulted in accurate gross sandstone thickness estimation, and ultimately improved volumetrics for risk analysis and reserve estimations.

Introduction

The explorationist is often exploring for oil and gas accumulations that reside in reservoir sandstones that are often less then 20 meters in thickness. This can become problematic when available 3D reflection seismic data are unable to resolve the vertical dimensions of such reservoirs, and can represent a hindrance when attempting to seismically predict gross rock volume for hydrocarbon reserve estimations. Such estimates represent a critical component to the overall derisking of the prospect inventory when short-listing prospective drilling locations. When bed thickness exceeds the resolving power of the seismic data, the explorationist may resort to alternative means such as probabilistic-type statistical methods in extrapolating / interpolating thickness measurements away from wells. This can be particularly challenging say, for example, in underdeveloped fields where well control is sparse and sand depositional environments are laterally heterogenic characteristic of more fluvial-type settings. Thickness prediction in developed fields incidentally can become difficult if reservoirs are structurally complex due to intense faulting, resulting in compartmentalization, and perhaps depositional expansion of reservoir beds. In such cases, correct thickness measurements of thin beds may not be captured do to infrequent lateral sampling between wells. Which ever the case, the inability of the seismic resolution to vertically resolve thin bed reservoirs adds to the quandary and associated risk of aggregate thickness prediction.

There is however, a phenomenon that occurs seismically when non-resolvable thin beds are encountered that may be effective in providing valuable information when attempting to estimate aggregate thickness. Once the resolving limit of the seismic as been reached, reflection amplitudes from the top and base of an arbitrary thin bed begin to spatially interfere with one another in a constructive manner, ultimately resulting in a derivative composite reflection amplitude. The amplitude interference between the two reflections continues to increase in magnitude as the bed continues to thin well below the resolvable limit of the seismic data. In fact, the increase in composite amplitude is linearly proportional to the thinning of the bed, a phenomenon known as *amplitude tuning*. The functionality of which was first assessed by Widess (1973) who observed that thickness information of a non-resolvable thin bed can be encoded in its resultant composite amplitude. Thus, valuable reservoir information can be extracted from the composite amplitude; a result of amplitude interference that would otherwise be deemed as seismic noise and a hindrance.

So how do we go about defining a thin bed? The answer lies in the seismic data resolution, defined by what is termed the ¼ wavelength tuning thickness which determines the minimal separation of two discrete boundaries the seismic data is capable of *resolving*, absent of any amplitude interference effects indicative of true amplitude response. Beyond the threshold of ¼ tuning thickness, interference effects begin to inundate amplitude, rendering top and base measurements of a bed inaccurate, at which point the "thin bed" can only be seismically *detected* via tuning amplitude.

A methodology in acquiring aggregate thickness directly from seismic tuning amplitude has therefore been defined in hopes of exploiting the functionality of such data from the deep gas trend of Tuscaloosa (defined below) where reservoir sandstones are predominately below ¼ wavelength tuning. The robust method involves a quantitative approach in transforming 3D reflection seismic data to an equivalent aggregate thickness cube allowing for the extraction of thickness information at each of the seismic traces. Key to the success of the method is the accurate inverse modeling of the linear relationship that exists between the tuning amplitude and thin beds below ¼ tuning thickness. This is achieved through the calibration of a *tuning model* defined by aggregate thickness from wells as a function of seismic tuning amplitude, resulting in a linear function simulating the tuning linearity. Converting tuning amplitude to a thickness domain did present a (uniqueness) quandary however, in that seismic amplitude is innately a non-unique measured quantity with no dimensions, deeming it difficult to define dimension-wise, which proved problematic when an effective thickness prediction method was being developed. The problem of non-uniqueness was indeed overcome by inverting the tuning amplitude in retrieving impedance, as a function of seismic reflectivity, through a constrained seismic inversion process; the accuracy of which was critical to the success of the method.

The utility and associated risk of our method was tested using 3D seismic and well log data acquired from the prolific deep gas Tuscaloosa trend, located in southeast Louisiana, USA. The trend is characteristic of over pressured and high temperature sandstone gas reservoirs at depths approaching 7000 meters, and represents some of the deepest onshore gas wells in North and South America. Sandstone reservoirs have been regionally tied to over 120 wells verifying seismic stratigraphy in collaboration with regionally interpreted depositional concepts. The accuracy of the tuning model has been tested at 24 blind well locations where aggregate sand thickness estimations have been acquired, and tested against true thickness measurements. An additional 13 "phantom" sands were successfully predicted below ¼ tuning thickness for a total of 37 predicted sands throughout the trend. The successful prediction of "phantom" sands demonstrates that the method is robust in predicting sands not indigenous to the tuning model. Overall, the results are encouraging and show that the model is accurately predicting sand thickness away from the wells which is confirmed from blind well measurements.

The accuracy of the method will ultimately reflect the precision at which the tuning model was calibrated; the correctness of which is reflected in the linear function which is ultimately tied to the wells and seismic data. Although the method is robust, successful implementation does require a full understanding of the seismic theory and processes involved, as well as the required data preparation. A tutorial is presented to further familiarize the reader with theoretical concepts as to the physical origins of seismic reflection events, and the inverted processes involved in extracting rock properties from such events. A thorough realization of these concepts is vital in understating the inner workings of tuning phenomena, when extracting thin bed thickness from tuned seismic impedance.

Theory of Exploration Seismology

Reflectivity

The seismic reflection method deals with the measurement of propagating acoustic waves through the earth, and involves the subsequent behavior of such waves as they pass through layers of rocks and fluids with contrasting rock properties. When the propagating wavefront encounters an interface of a stratigraphic layer of dissimilar rock properties and/or fluid saturations, a seismic reflection occurs whereby a fraction of the propagating incident acoustic energy is reflected back to the surface were it is recorded in the form of a sinusoidal wavelet (or seismic trace) containing amplitude and frequency information. The remaining portion of the wavefront energy, not reflected, is transmitted to deeper substrata where additional stratigraphic contrasts are encountered resulting in further reflections, also termed *seismic events*. Consequently, this ratio of reflected to transmitted energy is represented by what is termed the rock's *reflectivity r*, and is defined by:

$$r = \frac{A_r}{A_i}, \qquad (1)$$

where the magnitude of r is proportional to the reflected energy represented by amplitude A_r to that of the initial propagating wavefront energy defined by its amplitude A_i. It can be observed that as the rock property contrasts between two layers increases, so does the seismic reflectivity at their separating boundary resulting in larger values of A_r. The measurement of reflectivity, the magnitude of which is represented by seismic amplitude, is interpreted by the explorationist in inferring subsurface geology including structure and potential reservoir properties when seismically prospecting for hydrocarbons. Frequency information, innate to the seismic traces is also recorded at the surface with reflection amplitude and defines geometrically the thickness a layer must be to allow for accurate interpretation of its top and base. This concept is referred to as *seismic resolvability*, which is layer and depth dependent, and will be discussed later in greater detail.

The magnitude of A_r defined above can also be looked at as a measurement of *relative* dissimilarity between an arbitrary

contrasting layer and its encasing rock (e.g., sand encased in shale). Because reflectivity is represented by a ratio, it is a dimensionless value; the magnitude of which is only relative to the encasing rock, and as such, presents a non-unique representation of measurement. This can become cumbersome when trying to define rocks in terms of physical meaning that can be conceptualized stratigraphically when interpreting. A manipulation of the seismic data termed *seismic inversion* attempts to overcome this quandary by inversely extracting the reflectivity from seismic amplitude resulting in measurements with tangible units.

Rock property and fluid contrasts of stratigraphic layers in the earth give rise to reflectivity that may result in interpretable seismic events containing geologic information encoded in the reflection amplitude. Seismic reflectivity can be a source of analytical information in predicting rock properties that have been calibrated and tied to well logs. The seismic amplitude response (minus noise and multiples) can be intrinsic of rock physics in defining what is referred to as the rock's bulk modulus. The modulus is defined by the integration of three first order variable components 1) the rock's mineral assemblage and lithology, 2) the rock's framework comprised of properties such as density, porosity and texture related variables, and 3) the fluid density of pore space fluids which can include any mixture of formation water, gas, or oil. Examples of second-order variables that may induce a seismic amplitude response include, but are not limited to, reservoir temperature and pressure, steam, and varying levels of CO_2 within the reservoir rock. This information may be beneficial in assessing subtle amplitude changes associated with 4D seismic as recovery strategies evolve.

Any combination of these aforementioned variables, either first or second order, contribute to the overall magnitude of a rock's bulk incompressibility, a measure of rigidity defining a rock's compressional *p-wave velocity* (or pressure wave velocity) which is characteristic of the rate at which the acoustic wavefront propagates through the earth. The p-wave velocity of a rock is related to the bulk modulus given by:

$$Vp = \sqrt{\frac{K}{\rho}}, \qquad (2)$$

where V_p is p-wave velocity, K the elastic bulk modulus, and ρ the rock's bulk density.

Conceptually, as the rigidity of a rock decreases, say stratigraphically from shale to reservoir sands for example, so does its p-wave velocity, an effect likely attributed to an increase in porosity inherent of the sand; an increase in porosity softens the rock. Or conversely, brine can replace a saturating gas, increasing the rock's fluid density, resulting in a less compressible or more rigid medium induced by the brine, thus increasing the rocks bulk modulus and hence, p-wave velocity.

Rock properties mentioned above are interrelated, and the delineation of the seismic response to any of these properties can be problematic. The fluctuation of one property, or combination of properties, can induce a similar seismic response, resulting in non-unique solutions. This problem can become critical when attempting to estimate properties from seismic amplitude alone. However, these non-unique solutions can be minimized via the forward modeling of the seismic response constrained by well log measurements.

Acoustic Impedance

A rock's compressional p-wave velocity contains critical information that can be extracted from seismic amplitude when analyzing prospective reservoir rocks. Contrasts in p-wave velocity, coupled with bulk density, define seismic reflectivity, and therefore can be determined at stratigraphic boundaries the reflection amplitude originated from. Hence, if we recede inversely and extract the seismic reflectivity from reflection amplitude, valuable information can be obtained. This is an inversion process that becomes more conceptually apparent when *reflection coefficients* are considered. A reflection coefficient equals reflectivity, but with different terms. Here the ratio of reflection amplitude to that of the incident amplitude, defined in equation 1, is now replaced by a ratio as a function of impedance contrasts and differences that are inherent to the opposing layers at their boundary according to:

$$RC = \frac{\rho_2 v_2 - \rho_1 v_1}{\rho_2 v_2 + \rho_1 v_1}, \qquad (3)$$

where *RC* equals the reflection coefficient, ρ the bulk density, and *v* defines p-wave velocity of the rock. Subscripts one and two refer to the opposing top and bottom layers, respectively, as depicted in figure 1 (panel 1). The separate quantity of *v* times ρ intrinsic of each layer equals a physical rock property referred to as *acoustic impedance*, which is innate to that layer. It can be observed from the above equation that the reflection coefficient represents a ratio of acoustic impedance contrasts at the interface of opposing layers. As the impedance contrast between two layers increases in magnitude, so does the reflectivity, and hence, the resultant amplitude. Analogous to reflectivity, the magnitude of the reflection coefficient is dimensionless and measurements are non-unique.

It is important to note that the sign (plus or minus) of the reflection coefficient and reflectivity depends on what is referred to as the *seismic polarity*. For example, a seismic trough (as opposed to a peak) more commonly represents a decrease in seismic impedance (Figure 1, panel 2), which physically translates to a softer, less rigid rock overlying the harder rock. This would be the case if encountering a transition from shale to porous sand. Here, the resulting reflectivity / reflection coefficient would have a negative sign and would be seismically represented by a trough equivalent to relatively lower values of impedance. Variations in amplitude could be interpreted as changes in rock properties, or porosity in this case. The opposite response is true if a relatively harder rock is encountered, say from a shale encased in porous sand. In this case a positive reflectivity would result,

indicative of a seismic peak or a *reversed polarity*.

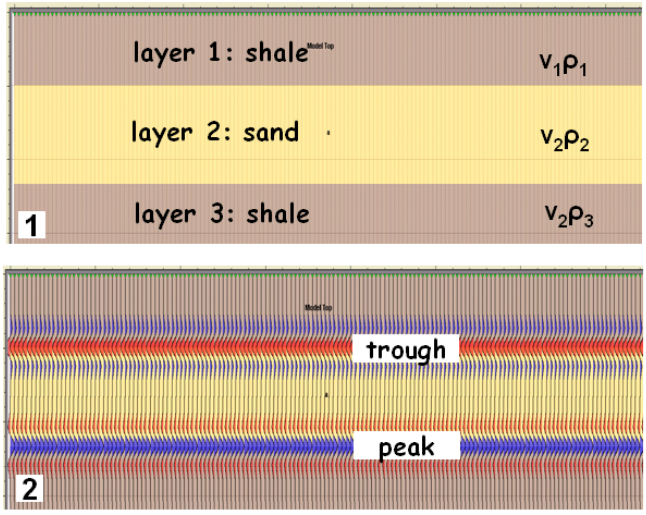

Fig. 1. A three layer model of a low velocity porous sand encased in a high velocity non-porous shale, where $V_1 = V_3 > V_2$. The resultant seismic response is shown in panel 2 characteristic of a minus-plus (trough-peak) polarity.

Seismic Stratigraphy

The reflection coefficient defines amplitude variations in terms of physical rock properties as opposed to reflectivity which is defined as a function of propagating wavefronts. P-wave velocity and bulk density, expressed as acoustic impedance, represent quantities that can be measured in situ by well logs, and velocity which can be sampled directly from core data in the lab at ultrasonic frequencies. If logs are available, an acoustic impedance log can be obtained by simply multiplying the reciprocal of the p-sonic log (equivalent to p-wave velocity) by the bulk density log. The acoustic impedance log can now be directly "tied" to the relative seismic amplitude; a meticulous process that establishes seismic stratigraphy by calibrating the seismic events in time to acquired well logs in depth. Seismic-to-well ties (Figure 2) play a critical role when transferring stratigraphic depositional concepts, interpreted from well logs and cores, to seismic events. This method is termed *seismic stratigraphy*, a discipline which attempts to define depositional environments via interpreted seismic data. This requires the accurate aligning of interpreted stratigraphic intervals with corresponding seismic events.

The precision of well-to-seismic ties represents the foundation that ultimately determines the success of any seismic interpretation study, both stratigraphic and structural. This can become especially problematic when seismically extracting thickness information from tuning amplitude. As we will see later, bad well ties will result in erroneous thickness estimations because the seismic tuning model, specific to a particular sand layer, is calibrated to sand thickness representative of geologic well picks. The correlated seismic tuning amplitude is subsequently tied to those same picks. If the well-to-seismic tie is in error, seismic amplitude representing the wrong seismic event will be analyzed when predicting thickness; a method that will be clarified in the next section. An additional pitfall from bad well ties may arise when incorrect seismic rock properties innate of amplitude are extrapolated / interpolated away from calibrated wells when probabilistic-type modeling is being implemented. Obviously, if the seismic is incorrectly tied to the well, false amplitude information will be representing the wrong stratigraphic layer, which will then in turn be erroneously interpolated away from the well when populating geologic models. Therefore, in avoiding bad ties, a common practice entails the forward modeling of synthetic traces nearest the wellbore. This is a subject involving an iterative process of zero-phase wavelet estimation, and the convolution of such wavelets with an earth reflectivity series representative of impedance well logs and cores.

An example from the Tuscaloosa trend of southern Louisiana shows the desired precision of a tie, shown in Figure 2. Here, seismic traces nearest the wellbore (panel 1) have been tied to the impedance log (blue curve, panel 4) representative of real earth reflectivity, which has been filtered back to seismic bandwidth for scaled correlation. Panel 3 shows the inverted impedance extracted from the traces shown in panel 1.

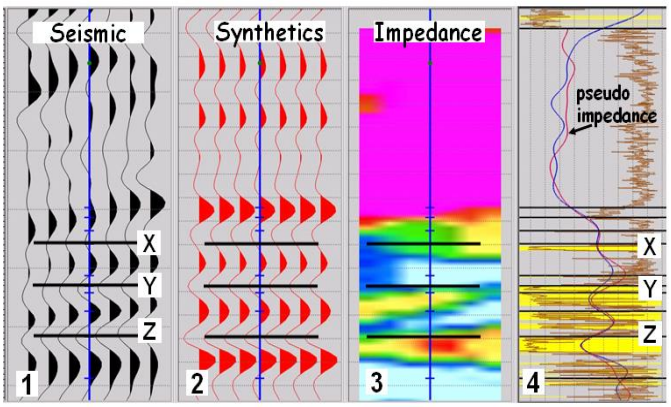

Fig. 2. An example of a seismic-to-well tie showing stratigraphy concepts calibrated to seismic amplitude. Notice the inverted impedance (panel 3). Yellows and blues are sands and shales, respectively. Sand Z is indicative of tuning and is brighter and thicker relative to sand X which is also tuned but is dimmer and thinner. Sand Y is above ¼ tuning thickness and measures true thickness.

The gamma ray log (brown curve, panel 4) measures formation radioactivity, and identifies the stratigraphic intervals with the sandstones highlighted in yellow. Rock property analysis (described below) confirms that the blocky highly porous sands are characteristic of slower p-wave velocity and bulk density, relative to the high velocity encasing background shale. First, notice the impedance log response (blue curve) to lower values of impedance upon the onset of the more porous sand (pick X), relative to the background shale. The log signature (to lower values of impedance) is repeated two additional times throughout the zone of interest, characteristic of deeper sands (picks Y and Z) that possess similar rock properties. This therefore intuitively should result in an equivalent series of negative reflection coefficients. We should therefore expect a sequence of seismic troughs characteristic of negative reflectivity that align with

the sands, which is indeed the case (panel 1). Also, in panel 3, we see that the inverted impedance from the real seismic (panel 1) ties satisfactorily; low impedance values (yellow and green colors) physically agree with the more porous compressible sands, and high impedance (blue colors) correspond to more rigid less porous shale. Also, notice the perturbation of unusually low impedance values (red color), indicative of sand Z.

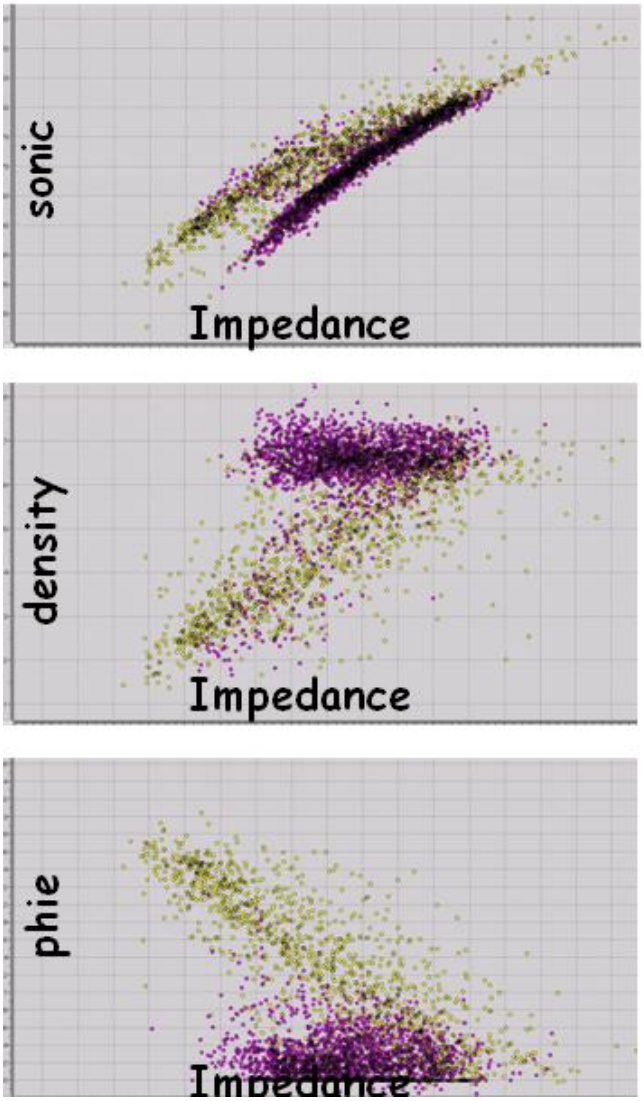

Fig. 3. Cross plots show where sand (yellow) plots relative to background shale (purple) as a function of impedance. This analysis assesses the potential functionality of extracting rock properties from seismic amplitude.

This is incidentally the result of *tuning* as is characteristic of sand X as well. Incidentally, sand X will be the reservoir sand that tests the prediction accuracy of the *tuning model* described in the next section. The seismic data is effectively resolving the top and base of sand Y. Lastly, the synthetic traces in panel 2 show good agreement with the real seismic data nearest the wellbore, confirming the correct zero-phase wavelet response (in time) to the earth reflectivity in depth. This is confirmed when we extract an inverted pseudo-impedance log (red curve) directly from the seismic data and compare its shape to the existing impedance log (blue), which shows an excellent tie in this case.

The calibration of well impedance logs (sonic and density) to seismic amplitude enables the creation of empirical rock property relationships. This enables the explorationist to seismically predict such properties away from wells. This straightforward form of rock property analysis is recommended before the commencement of any stratigraphic interpretation in measuring the functionality potential of amplitude induced rock property changes. Figure 3 shows cross plots of velocity, bulk density and effective porosity as a function of well log impedance, and defines where sand plots relative to encasing background shale as a function of impedance. The yellow and red colors distinguish porous sand from shale, respectively, which has been determined from gamma ray log measurements. Panel 1 shows a population of sonic (p-wave velocity) points, that plot to the left of the shale trend inferring that the overall bulk compressibility of the sand is less then the encasing shale. Thus, in this case the plot confirms that sand is characteristic of lower p-wave velocity then shale. Bulk density (panel 2) on the other hand plots further away from the shale suggesting density may be more of a diagnostic lithology indicator then velocity. Finally, plot 3 indicates that higher porosity sand, with lower impedance, plots to the left of the shale trend. Also notice the linearity at which the points increase in porosity with decreasing impedance, which is typical of a seismic response to increasing porosity. Thus, all three plots suggest that the seismic amplitude (or impedance) should be able to distinguish higher porosity reservoir rock from non-porous shale. That is, if key seismic events have been precisely calibrated to the correct stratigraphic layers from which the cross plots represent.

Poor ties can have significant ramifications to any seismic interpretation project and may include: inaccurate structural predictions, erroneous trap definition, mis-positioning of faults, and poor juxtaposition and seal analysis. Poor ties and the resulting interpretation can ultimately lead to inaccurate prospect volumetrics and reserve estimations. Precise well-to-seismic ties require a thorough physical understanding as to the many variables, and combinations of such variables, that may give rise to a seismic reflection. This isn't always a straight-forward process, and a "good" tie, with aligned events and near perfect synthetics, doesn't necessarily represent a correct tie if the seismic response remains unknown. The reader is referred to Shoemaker, et al (2006) for a well-to-seismic tie review and associated interpretation pitfalls thereof.

Full Bandwidth Seismic Inversion

It has been shown above that the reflection coefficient defines seismic amplitude in terms of physical rock property contrasts (i.e., velocity and density), as opposed to its equal counterpart, reflectivity. However, both representations of the amplitude response remain non-unique in that their ratios contain no units of measure. The seismic inversion method (an example of which is shown in figure 8) attempts to remove this ambiguity by going one step further in transforming seismic

data from the relative amplitude domain to the absolute impedance domain. The result is *full bandwidth* inverted seismic impedance that has equivalent well log impedance units, and bridges the gap between wells and seismic data. Inverted seismic impedance can be directly interrelated with existing rock physics concepts and depositional models derived from well log data.

The seismic inversion method provides additional utility which stems from the fact that the transformed inverted data are now full bandwidth; that is the inverted data includes frequencies from the lower end of the frequency spectrum. Conventional seismic data is inherently band limited usually from 5 to 10 Hz at the low end of the frequency spectrum, out to a maximum frequency between 20 and 50 Hz. The higher frequencies are more subsurface dependent to such variables as signal absorption and depth. In addition to the dimensionless quandary related to amplitude, conventional seismic data can be presented as a non-unique quantity due to the absence of these low frequencies. There isn't much that can be done in increasing the upper ended frequencies due to wavelet dependencies inherent to the source wavelet at the time of acquisition, however, the lower frequencies can be estimated from a priori sources such as impedance logs. In a comprehensive process, the well log impedance, representing a low frequency trend, is interpolated away from the wells resulting in an impedance cube that is ultimately merged with the band limited inverted seismic data. The impedance trend acts as a low frequency drift correction constraining the interpretation. Once the impedance cube is merged, a full bandwidth inversion solution results (e.g., 0 to 30 Hz), which minimizes the ambiguous nature characteristic of the band limited data. An additional advantage when interpreting inverted seismic is that the data are now presented as physical layers that resemble stratigraphic beds as opposed to interfaces inherent to conventional seismic data. For a comprehensive review of the seismic inversion method, the reader is referred to Latimer (2001), and Soroka and Shoemaker (2003).

Thin Bed Prediction from Tuning Impedance

Reservoir Volumetrics

Reservoir geometry and aggregate bed thickness predictions of oil and gas reservoirs play a vital role in the calculation of volumetrics when determining existing and prospective hydrocarbon accumulations. Such estimates represent a critical component to the overall derisking of the prospect inventory when short-listing prospective drilling locations, and are dependent upon a quantity referred to as the gross rock volume or GRV. The GRV is simply a product of the area (A) that is believed to contain the hydrocarbon accumulation times the aggregate (gross sand) thickness of the potential reservoir (H) expressed as:

$$GRV = AxH, \quad (4)$$

which is defined in cubic dimensions. When estimating hydrocarbons initially in place, the initial GRV is multiplied by correction factors that are characteristic of the reservoir such as the net-to-gross ratio, porosity, hydrocarbon saturation, and the formation volume factor of the oil or gas. These factors reduce the estimated GRV to corrected reservoir conditions, and are typically predicted using a combination of probabilistic and deterministic methods; the latter of which relies on statistics in populating subsurface models away from wells with data supplied by logs and core. Deterministic rock properties and seismic frameworks, inherent to seismic amplitude, are often used to constrain the populating of such models laterally between wells. Once these data are modeled, the initial GRV is corrected for using the above parameters. Appropriate reserve ranges are then estimated and economically assessed.

Thus, the initial GRV, prior to any corrections, represents a critical starting volume that, if estimated incorrectly, could result in significant errors when predicting hydrocarbon reserve ranges. This further emphasizes the accuracy of which the area (A) and the aggregate thickness (H) are determined in calculating the geometry of the GRV. Common practice is to first estimate, via 3D seismic, the interpreted surface area corresponding to the structural height component of the trap. The accuracy of this measurement is ultimately dependent upon well-to-seismic ties (a topic defined above), coupled with seismic data quality. Second, the area is multiplied by vertical aggregate thickness, which can be determined from the seismic data. Determining thickness can become more problematic, however, if the reservoir is thin beyond the vertical resolving power of the seismic data (a topic defined below). In such cases, a phenomenon known as reflection *amplitude tuning* can be implemented in predicting thin bed reservoir sand thickness, an objective that defines this study.

Vertical Seismic Resolution and Amplitude Tuning

When exploring for hydrocarbons in reservoirs that are usually no more then 20 meters thick, the available seismic data may not be capable of resolving vertically the top and base of such beds when determining aggregate thickness. When bed thickness exceeds the resolving power of the seismic, the explorationist may resort to alternative means such as probabilistic-type statistical methods in extrapolating thickness measurements away from wells. This can be problematic when depositional environments for example, are more heterogenic between wells characteristic of more fluvial-type environments, or if the reservoir is faulted resulting in compartmentalization and depositional expansion. In such cases, correct thickness measurements of thin beds may not be captured do to infrequent sampling, which may result in poor GRV estimates. The *seismic resolution* will often determine how thin a bed can be resolved, and hence, which method is most suitable when predicting aggregate thickness.

The seismic resolution can be expressed in practical terms according to its degree of functionality to *resolve* or *detect* a thin bed. The *resolving* of a thin bed means that the seismic resolution is capable of imaging separate contrasting impedance boundaries corresponding to the top and the base of the bed, and that the refection amplitude response of such beds are separate and do not spatially interfere. This degree of resolution allows for the continuous lateral mapping of the

physical top and base of a bed via seismic events in creating what are termed isochron maps, representing bed thickness variations as a function of time. For thinner beds however, only the presence of the bed can be *detected* from seismic amplitude, as the seismic data is unable to sufficiently separate or image the contrasting top and base impedance boundaries of the interface. Once the resolving limit of the seismic as been reached, reflection amplitudes from the top and base of a thin bed begin to spatially interfere with each other in a constructive manner, ultimately resulting in a composite amplitude. The amplitude will continue to increase in magnitude linearly as the bed continues to thin as it approaches zero thickness, and is said to be tuned at this point.

The concept of tuning is best illustrated with the aid of a *tuning wedge* which forward models the seismic amplitude response of a thinning geologic feature in defining seismic resolution. Figure 4 shows a stratigraphic example of a tuning wedge that is modeling the amplitude response (panel 2) of a thinning softer sand of low impedance (layer 2, panel 1) encased in relatively hard shale of high impedance (layers 1 and 3). Lithologic details of the model are irrelevant at this time, but the model does assume that the p-wave velocity V_1 of the top shale is greater then that of the p-wave velocity V_2 of the sand wedge, and equal to the bottom shale V_3, where $V_1 = V_3$ and is greater then V_2. The model was created by using a 25 Hz zero-phase Ricker wavelet that was convolved with the two term reflectivity series characteristic of the three contrasting layers. The vertical separation from the top and base sand equates to a trough to peak separation (or minus-plus polarity), and defines thickness as a function of two-way travel time. Below the tuning wedge (Figure 4, panel 3), is a quantitative plot referred to as a *tuning curve* which analytically displays various curves that measure the amplitude (defined as a function of reflectivity) of the thin sand bed response (curve a), the true thickness of the sand wedge (curve b), and the apparent thickness separating the top and base reflections of the sand (curve c).

Starting from the right side of the wedge, we see that the sand is at its maximum true thickness which is equivalent to the apparent thickness defining the trough to peak separation of the seismic traces. This is shown in Figure 4, panel 3, where the apparent thickness and true thickness curves (c and b, respectively) are identical and overlap. The trough and peak amplitudes (or reflectivity) in this portion of the tuning wedge are adequately separated spatially, restricting any amplitude interference. Thus for the top of sand, the relative seismic trough (negative reflectivity sign) is a true amplitude response to the impedance contrasts of the rigid shale to that of a softer porous sand. The opposite is true for the base of the sand where the shale is reencountered, and is represented by a seismic amplitude peak (or positive reflectivity sign). Because the rock properties of the shale are assumed to be constant through out the model, the magnitude of reflectivity relative to the top and base of the sand represents equal amplitude, that is opposite in sign and hence polarity (concept of polarity was described in the previous section).

As the wedge thins to the left, amplitude continues to measure changes true to rock property variations and/or fluid changes indicative of reflectivity as opposed to interference (or noise) induced amplitude. Furthermore, two-way travel time separation from trough to peak is accurately representing bed thickness that can be straightforwardly converted to depth if the p-wave velocity is known. Therefore, it can be said that the seismic data is successfully resolving the top and base of the sand throughout this portion of the wedge. This is also confirmed by the apparent and true thickness curves (curves c and b, respectively) that continue to overlap. That is, until point 1 is reached, where the amplitude begins to increase to higher negative values, as the onset of interference begins, and continues in intensity as the distance between trough and peak amplitudes decreases and the reflections become increasingly squeezed.

The Tuning Threshold

As the wedge continues to thin left of point 1, we see that the magnitude of amplitude interference, between the top and base reflections, continues to brighten (panel 2) until a specific true thickness (curve b) is reached that corresponds to an amplitude maximum (curve a, point 2). Here, the time distance between the trough and peak events has reached a physical minimum, resulting in a maximum composite amplitude; the result of interference. The maximum minimum thickness, where the amplitude maximum occurs, represents a common threshold when defining seismic resolution, and is referred to as the *¼ dominate wavelength tuning thickness* as defined by Raleigh (Jenkins and White, 1957), and is consistent with the p-wave velocity and frequency used for this particular tuning wedge model.

This quantity defines the absolute minimal true thickness a thin bed can be while possessing visible discrete reflections indicative of the top and base. This is further confirmed by comparing the thickness curves (b and c) that intersect at the amplitude maximum (point 2). Here, the point of intersection represents the thickness (or separating distance) at which point the trough and peak reflections can no longer be physically squeezed any closer, a limitation that is frequency intrinsic of the seismic wavelet. To the left of the amplitude maximum, as true bed thickness approaches zero past point 3, the apparent thickness (curve c) of the trough and peak remains unchanged and is constant, and thus no longer provides thickness information, which presents a quandary that provides a valuable tradeoff in the form of amplitude tuning.

As the wedge thins past the point of ¼ wavelength tuning, amplitude begins to decrease (as a function of reflectivity) from the maximum, and then becomes more linear (around point 3) which represents an additional threshold defining seismic resolution, and is referred to as the ⅛ *dominate wavelength tuning thickness* as defined by Widess (1973), and represents a point at which aggregate thickness can be estimated from the composite amplitude alone.

Thin bed reservoirs inherently below ¼ wavelength tuning therefore can not be seismically *resolved* in terms of a top and base, but may be *detected* if tuning information is available. Tuning involves the extraction of absolute thickness

information encoded within the tuned amplitude that would

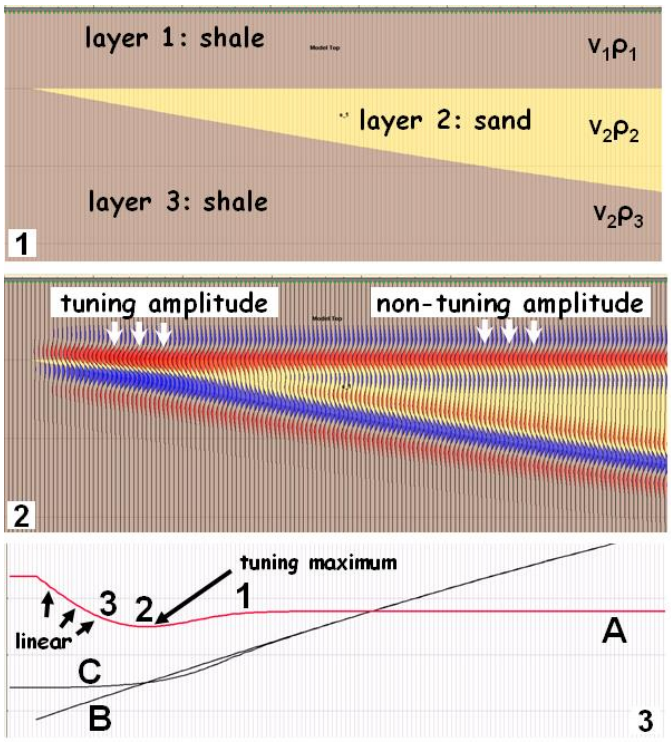

Fig. 4. The tuning wedge model represents a low velocity porous sand encased in a high velocity non-porous shale, and defines seismic resolution. The seismic response to the wedge is shown in panel 2, and illustrates the brightening of the tuning amplitude and its linear relationship as a function of true thickness (curve b, panel 3).

otherwise be considered a hindrance and dismissed as interference noise. For our tuning wedge model, the tuning effect becomes more visible as the amplitude of the top of sand brightens (Figure 4, panel 2) in response to interference. As the wedge continues to thin left of the amplitude maximum (curve a), we see that the amplitude curve linearly decreases proportionally with true thickness of the wedge to a point where amplitude eventually dies out at zero thickness. It is within this zone of linearity that thickness information can be obtained that is less then ¼ wavelength tuning resolution.

Tuning can be linearly expressed by an equation first proposed by Widess (1973) where *b*, the composite amplitude from tuning interference, is approximately proportional to the thickness of the bed and inversely proportional to the seismic wavelength expressed as:

$$b = \frac{4\pi ard}{\lambda_d}, \qquad (5)$$

where *a* is the amplitude of the incident wavelet, λ_d the dominate seismic wavelength, *d* is the thin bed thickness, and *r* equals the reflectivity / reflection coefficient without tuning and is referred to as *background reflectivity*.

Widess assumed that the rock above the thin bed was identical to the rock below which resulted in reflection coefficients of equal magnitude and opposite polarity; a case identical to our tuning wedge presented herein, where the model represents a measurement of low p-wave velocity porous sand encased in a high velocity non-porous shale. He also observed that as the distance (or thickness) between reflectivity of the top and base of a thin bed decreased, interference resulted in a composite amplitude waveform at which point the wavelet stabilized and trough to peak time-distance remained constant, while amplitude continued to increase as the bed thinned. Widess concluded that the point at which thickness could be extracted from amplitude occurs at ⅛ the wavelength of the predominate frequency, and states that thickness information may be determined for thin beds that are considerably less then ⅛ tuning thickness. Conclusions of Kallweit and Wood (1982) are similar to those presented by Widess in that below the ¼ wavelength tuning resolving limit, amplitude information is linearly encoded in the composite amplitude, provided the amplitude response is entirely the result of interference wavelet effects. This result permits bed thickness estimations provided the *in situ* thickness has been properly calibrated (i.e., optimal well-to-seismic ties). They also stress the importance of seismic data processing, presumably to preserve true amplitude response, and state that zero phase (processed) data are essential when defining reservoir dimensions from tuning amplitude. Voogd and den Rooijen (1983) confirm that for a certain wavelet (frequency) there exists a separate range of layer thicknesses that can be resolved (above ¼ tuning), and in principle, thickness can be determined from a "thin" bed using reflection amplitude below this limit. They also suggest (as does Okaya, 1995) that, if tuning information is desired, the seismic data may be processed accordingly to enhance tuning amplitude by decreasing the spectral bandwidth of the data, as opposed to processing-out the tuning amplitude, otherwise deemed as noise. Chungt and Lawton (1995) stress the importance of a zero-phase wavelet criterion in presenting a linear solution based on a Ricker wavelet approximation similar to Widess's equation, and show that above ⅛ tuning, thickness approximations are no longer valid. They also confirm the importance of calibration (ties) of wells to the seismic amplitude as previously discussed, thus reemphasizing the importance of correctly calibrated seismic stratigraphy to wells.

Inverted Tuning Impedance

Amplitude response in the case of tuning is due to reflectivity (or reflection coefficients) primarily induced from interference / geometric effects of the top and base of the thin bed, not so much by impedance contrasts resulting from rock property and/or fluid saturations, effects of which can now be considered background amplitude. It can be said that amplitude response of tuning is the result of *"tuning reflectivity*", the byproduct of tuning interference effects, and subsequently represents a measurable quantity that can be inversely extracted from the seismic data via inversion (a topic discussed in the previous section). If inverted tuning reflectivity measurement can be obtained so can thickness information linearly inherit to such data, so long as the composite amplitude response is the result of tuning effects at ⅛ tuning thickness, and not some other type of noise. This is

further substantiated by showing that tuning reflectivity of the tuning wedge (extracted from curve a) verses true thickness (curve b) is a linear function (Figure 4, panel 3). This can be expressed by rearranging the terms of equation 5**,** substituting r_t for *b*, and solving for the gradient which yields:

$$\frac{r_t}{d} = \frac{4\pi a r}{\lambda_d}, \qquad (6)$$

where r_t equals *b*, which is the tuned reflectivity of the composite amplitude. Figure 5 plots tuned reflectivity of the composite amplitude verses true thickness. Below the amplitude maxima, the reflectivity begins to decreases to the right as we approach ⅛ tuning thickness where the true thickness becomes linearly proportional to reflectivity, the gradient (or slope) of which is defined by r_t / *d*. Incidentally, the non-tuned reflectivity *r* (or background reflectivity) in the above equation represents the initial onset of the reflectivity minus any tuning effects, which is observed at thicknesses greater then ¼ tuning. As we will see in the next section, this background reflectivity acts as a factor in limiting the dynamic range of tuning linearity.

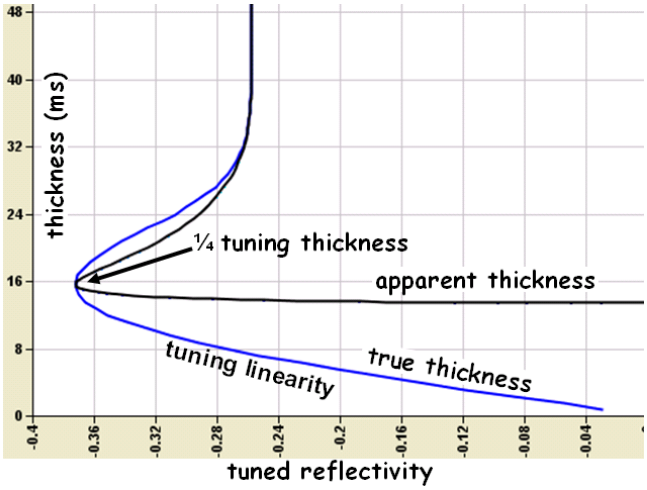

Fig. 5. A tuning curve showing the amplitude response of the tuning amplitude depicted in figure 4. The axes have been rotated to match the gradient (or slope) defined in equation 6 (and figure 6). The x axis equal to tuned reflectivity is representative of tuned seismic impedance, which linearly increases in magnitude to the left as the bed thickens.

The tuned reflectivity (figure 5), an approximation of the composite amplitude, is summarized as the variable that links the relative seismic data to physical aggregate thickness tied to well control. This has been analytically confirmed via the forward modeling of tuning effects using a tuning wedge with similar criteria proposed by Widess (1973), and others. The tuning wedge explicitly shows the linearity characteristic of true thickness versus tuning reflectivity; a quantity represented by reflection coefficients that can be inversely determined in the form of seismic impedance referred to here as "*tuning impedance"*. Because seismic inversion involves every trace, we now have thickness predictions densely sampled at each of these locations. The end result is an aggregate thickness cube that compliments seismic structure.

Defined in the following section is an example where we have successfully increased thin bed detection well below ⅛ tuning thickness, thus doubling unresolved seismic resolution by an order of magnitude, and show a practical real-world example of the methods utility applied to the prolific deep Tuscaloosa gas trend of Louisiana, USA.

Practical Application using Tuned Impedance

Methodology

We began our groundwork discussion with the generalized theoretical origins of seismic reflection amplitude focusing on reflectivity and its counterpart, the reflection coefficient. It was discussed that the reflection coefficient (defined as a function of impedance) more uniquely represents the reflection amplitude in terms of measurable quantities such as velocity and density of the rock, but nevertheless remains non-unique due to its dimensionless nature. Acoustic impedance attempts to minimize this ambiguity in defining seismic amplitude as a rock property that is defined in measured units by means of the seismic inversion method. Moreover, the inversion provides a more unique measurement by constraining the inversion solution using a low frequency trend interpolated from a priori data. The resultant solution is full bandwidth inverted impedance defined in units (of m/sec*g/cc) which can now be inversely converted to tuning reflectivity r_t, when approximating aggregate thickness defined below. For an example of the seismic inversion processing flow, the reader is referred to Soroka and Shoemaker (2003).

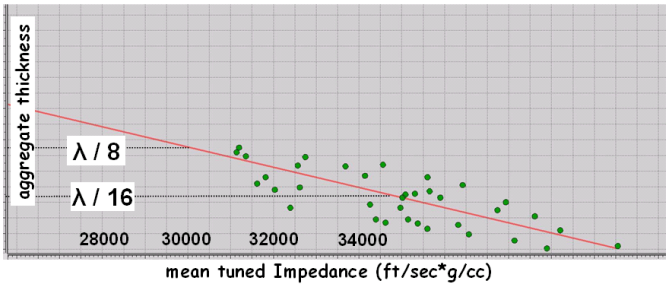

Fig. 6. The linear function defines the tuning model representative of Tuscaloosa, which has been calibrated to the seismic data as a function of real log thickness. Conceptually, the tuning model here is equivalent to the tuning linearity portion of the curve defined in figure 5. Notice the similarities between the two figures.

Equation 6 defines the gradient r_t / *d* that represents the linearity observed from the tuning curve (figure 5) as a function of tuning reflectivity r_t (which we are attempting to solve for seismically via inverted tuned impedance) and *d* the aggregate thickness. The gradient is proportional to the background reflectivity *r* and seismic wavelength λ_d, which are known quantities inherent to the seismic data. Variable (*a*) is approximated, and represents relative amplitude of the estimated zero-phase source wavelet.

When we examine the tuning curve of figure 5, we see that the onset of linearity begins below the ¼ wavelength tuning

thickness, where the maximum negative reflection coefficient is occurring. The linearity proceeds to less negative reflection coefficients as true thickness thins, and passes through ⅛ wavelength tuning thickness as the curve approaches zero. This tells us that just below ¼ tuning thickness, the amplitude trough of our tuning wedge model (figure 4) is at its maximum negative amplitude characteristic of the thickest sand, equivalent to a maximum lowest impedance value. The model tells us that as a bed's thickness increases toward the ¼ tuning limit, we expect tuned inverted impedance to inversely decrease to lower values (as depicted in figure 6). Therefore, in the case of this particular model, thicker sands (below ¼ tuning) are indicative of brighter seismic events characteristic of low seismic impedance. Before we can begin predicting aggregate sand from real data however, a *tuning model* must now be created that calibrates well log thickness linearly to tuned seismic impedance. For our example, we will be using well log and 3D seismic data that have been acquired from the deep gas Tuscaloosa trend.

Practical Application

The utility and associated risk of our method was tested using 3D seismic and well log data acquired from the prolific deep gas Tuscaloosa trend, located in southeast Louisiana, USA. The trend is characteristic of over pressured and high temperature sandstone gas reservoirs at depths approaching 7000 meters, and represents some of the deepest onshore gas wells in North and South America. The Tuscaloosa sandstones in the study area are Cenomanian in age and were predominantly deposited in a deltaic environment. Sediment loading, growth faults, and subsequent expansion affected the distribution and thickness of the sandstones throughout the trend. Intervals with more lateral continuous and "sheet-like" sandstones are inferred to have been deposited in a more structurally stable environment with relatively limited growth fault activity. The Tuscaloosa sandstones are remarkably porous for their depth of burial as the better sandstones can contain porosities of 25% to nearly 30% at depths near 7000 meters. Chlorite grain coatings and selective dissolution of rock fragments and carbonate cement can locally be major contributors to the current distribution of porosity.

Rock property analysis (figure 3) indicates that impedance linearly decreases with increasing porosity, and confirms that porosity values greater than 20% can be readily identified from the inverted seismic impedance; that is in areas not inundated with tuning noise. Tuscaloosa completions in such sand are characterized by unstimulated high initial rates (which range from 10 to 80 mmcfd). Initial reservoir pressures and temperatures range from 8,300 to 19,000 psi and 340 and 410 degrees F, respectively. The drive mechanism is primarily partial waterdrive with recovery factors between 50% and 70% of the original gas in place. The tuning model (defined below) has been calibrated to a deltaic sandstone reservoir (see figure 2, sand X) characteristic of "sheet-like" deposition as described above. Regional sequence stratigraphic concepts are consistent with well log interpretation confirming that the sand is regionally encased in thick shallow marine shales that act as sufficient overlying top seals. 3D seismic data has been recently reprocessed which has resulted in laterally consistent zero-phase data with amplitude preservation. Sonic logs, as well as interval velocities estimated from the 3D seismic, confirm that the reservoir sand is characteristic of lower p-wave velocity relative to the encasing higher velocity shale, which is consistent with the tuning wedge parameters discussed above. Key sandstone intervals have been regionally tied to over 120 wells, and seismically interpreted throughout the 3D survey. An example of one such tie is shown in figure 2. Amplitude and frequency spectra were also sampled at each of these ties to confirm lateral zero-phase and frequency consistency. Due to extreme depths, the zero incidence full stack seismic data quality at Tuscaloosa is generally poor (figure 8), which is predominately the cause of amplitude attenuation effects. Moreover, absorption of higher frequencies, caused by a regionally overlying thick 300 meter chalk, has likely further decreased seismic resolution. The principal hindrance though is that aggregate thickness of the reservoir sands are predominately below ⅛ tuning thickness. Tuscaloosa therefore represents an ideal medium to test the method.

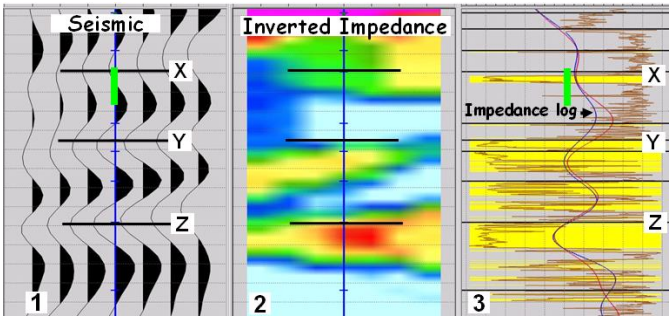

Fig. 7. An example of a seismic-to-well tie highlighting the vertical range (trough-to-peak) used to extract the tuned inverted mean impedance (green line) representative of sand X.

The Tuning Model

Critical to the successful transformation of seismic impedance to aggregate thickness requires the correct estimate of tuning linearity at ⅛ tuning thickness, which is characteristic of the tuning curve shown in Figure 5. The end result is referred to as the *tuning model*. This process involves the correct estimation of a linear function representative of the linearity portion of the curve which will be representative of input data related to rock proprieties specific to sand X and the encasing shale. This requires a procedure that accurately calibrates aggregate thickness from wells as a function of tuned inverted impedance information obtained from the seismic data. The slope of the function will be ultimately defined by r_t / d defined in equation 6, where r_t is approximated by tuned seismic impedance. The accuracy of sand thickness prediction will ultimately prove the precision at which the tuning model was calibrated; the correctness of which is reflected in the linear function.

The tuning model representing our Tuscaloosa sand is shown in figure 6, and was parameterized using 36 wells that were spatially chosen to adequately sample the trend-wise regional deposition of sand X. An example of one such well is shown in figure 7, which is identical to the seismic-to-well tie

example shown in figure 2. Reservoir sands have again been labeled X through Z, and the blue and red curves represent the real and pseudo impedance logs, respectively. The well impedance log has been filtered back to seismic resolution to allow for effective correlation with the pseudo impedance log that was obtained directly from the seismic inversion cube. All wells used to calibrate the tuning model have sand thicknesses (of sand X) well below ⅛ tuning thickness which is evident from figure 6.

The calibration of the tuning model involves the extraction of *mean tuned impedance* data from an inverted trace nearest each of the wells used in the model. An example pseudo impedance curve, from which the mean impedance was taken from, is shown in figure 7 (red curve), and represents an actual inverted seismic trace nearest the well bore. The mean of the impedance is taken from the onset of the top interface of the bed down to its base. The vertical range is defined from the maximum seismic trough to the maximum peak amplitude. The mean of the seismic impedance is then acquired between this vertical range which contains the encoded thickness information innate of the tuned amplitude. The mean tuning impedance value, characteristic of aggregate sand at this particular well, is defined by the green line superimposed with the pseudo impedance log (figure 7). Mean tuned impedance was acquired at the remaining well locations, and the values were plotted as a function of aggregate thickness in defining the linear function shown in figure 6.

Choosing the vertical range from which the mean impedance will be acquired is straightforward. As discussed in the earlier section, the trough and peak time distance at ¼ tuning remains constant as true thickness of the bed continues to thin. The separation should not appreciably decrease any further at other well locations if seismic frequency and p-wave velocity of the sand remain reasonably consistent. Any significant increase in the vertical tuning range may be indicative of thicker sands above ¼ tuning, in which case rock property and/or fluid induced amplitude changes will begin to interfere with tuning amplitude causing erroneous thickness predictions.

Results and Blind Well Test

The linear function (defined in figure 6) conceptually equals the linearity portion of the tuning curve depicted in figure 5, and provides a vehicle to directly transform tuned seismic impedance to an aggregate thickness domain defined in meters. An example of this application is shown in figure 8. The three 2D cross sections (representing a larger 3D cube) show the improvement in clarity from conventional seismic data (panel 1) to full bandwidth inverted impedance (panel 2) which was then transformed via the tuning model to aggregate thickness (panel 3). The three seismic horizons (X through Z) have been stratigraphically tied to the geologic picks defined in the example well tie shown in figure 2. Horizon X represents the top of sand X used in our example above, and remains below ⅛ tuning thickness throughout this 2D section; hence, any interpretable amplitude along this section is the result of tuning. Also shown are gamma ray logs from additional wells that have been filtered back to seismic bandwidth for easier correlation, and show the level of precision the sands have been tied to key seismic events. Panel 1 illustrates the high degree of noise characteristic of Tuscaloosa onshore seismic data, and the improved image the inversion (panel 2) provides. The contribution of the added low frequencies has enabled the events to be easier correlated laterally, resulting in significant improvements in both stratigraphic and structural interpretation trend-wise. The inverted seismic impedance is then transformed via a linear function, defined from the tuning model, to aggregate thickness (panel 3).

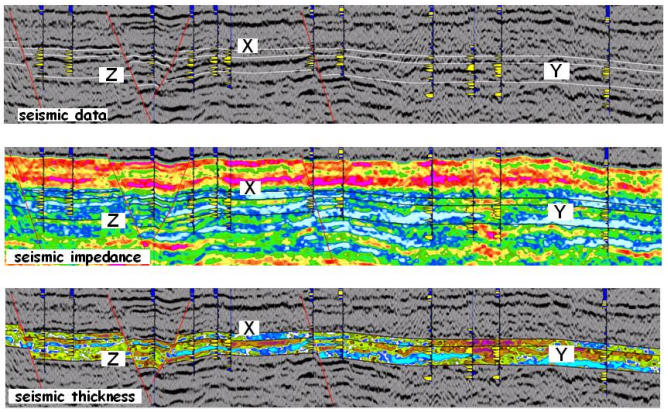

Fig. 8. 2D example cross sections of the seismic data (panel 1) showing data improvement from the full bandwidth inversion (panel 2), and the resultant transform to aggregate thickness (panel 3).

Aggregate sand thickness of panel 3 can now be directly obtained representative of sand X, where low measurements of seismic impedance from panel 2 (yellow and red colors) are characteristic of thicker sands (browns and purples) as confirmed from forward modeling of our tuning wedge. Blue areas define thinner sand (or areas of higher impedance), and may represent less prospective areas for gas (from a stratigraphic perspective). This may become especially apparent when volumetrics and hydrocarbon reserves are estimated using the predicted thicknesses. Area-wise horizon slices (figure 9) could be particularly useful when quantitatively predicting gross rock volume (GRV), as discussed in the prior section. Aggregate thickness information could now be acquired directly from a 3D aggregate thickness cube that represents densely sampled thickness measurements at every seismic trace location that may collaborate with structural geology, also defined from the seismic data.

The accuracy of the tuning model (figure 6) representing sand X, has been tested at 24 blind well locations where aggregate sand thickness estimations have been acquired, and tested against true thickness measurements. Of the 24 blind wells, 13 do not have sonic logs which were estimated empirically from nearby wells in acquiring pseudo checkshots for tieing. Density logs were estimated using Gardner's equation where needed. Also, 13 additional "phantom" sands (discussed below), stratigraphically unrelated to sand X, were successfully predicted below ¼ tuning thickness as well, for a total of 37 predicted sands. The criteria used in selecting the blind wells were comprehensive, and represent locations

throughout the trend to effectively assess regional thickness prediction in relation to lateral depositional inconsistencies, and include wells that would be classified as exploration as well as development.

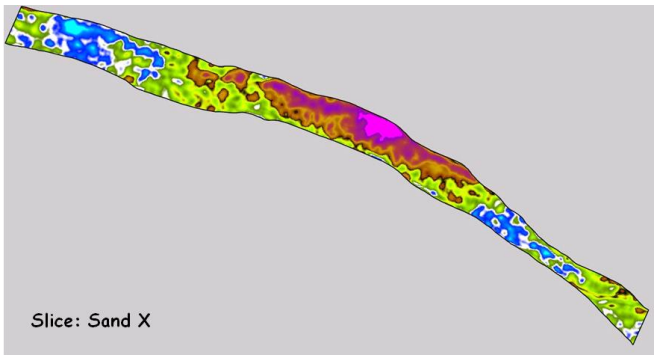

Fig. 9. An example thickness slice representative of the 3D aggregate thickness cube. Purples and browns are relatively thicker sands. Incidentally, maximum thickness (purple) collaborates with structure indicative of depositional expansion which has been confirmed from the well log data.

Predicting thickness information representative of sand X at blind well locations was straightforward, and involved the 3D thickness cube transformed from inverted seismic impedance via the tuning model (figure 6). Seismic converted "thickness traces" nearest each of the blind well locations were extracted, and thickness information representative to sand X was obtained. The majority of the predicted thickness points (highlighted blue) lie satisfactorily within the prediction curve (figure 10) where accurate sand thickness prediction is occurring well below ⅛ tuning, and could be argued that sand prediction is occurring near 1/16 of the wavelength as well. This could be explained from the addition of low frequency information provided by the full bandwidth seismic inversion which has also been observed by Hill (2005) who concluded that the use of impedance data substantially increases thin bed detection, compared to conventional seismic data. There are some outliers that plot away from the curve for reasons most likely attributed to amplitude noise intrinsic of the seismic data, processing artifacts, p-wave velocity and frequency inconsistencies, and perturbations in the background reflectivity which is discussed below.

Discussion

The Widess equation (1973) defines that the composite amplitude reflection from a thin bed (below ¼ wavelength tuning) is approximately proportional to the physical thickness of the thin bed, defined in equation 5. Alternatively, the composite amplitude can be looked at as a measured quantity representative of interference (or noise) resulting from the thin bed. As the top and base reflections of a thin bed get squeezed closer, the resulting interference increases proportionally as the bed thins; thus, the magnitude of interference can be looked at as a measure of thickness. As we showed, this measurement of interference can be expressed as "tuning reflectivity", which in turn can be approximated in a quantitative sense using seismic tuning impedance from the full bandwidth inversion process. The seismic tuning impedance in this case is not a first-order amplitude response to rock property induced impedance contrasts, but an "amplitude interference response" of the closely spaced thin bed reflections; the magnitude of which is a measure of interference which incidentally represents the source of linearity we wish to model in predicting thickness.

Although secondary-order to interference, reflectivity from rock property induced impedance contrasts inherent to the thin bed does in fact contribute to the overall composite amplitude, and represents the so-called background reflectivity equation 6 referred to earlier. This reflectivity represents rock property impedance contrasts as if the bed was thick to begin with, representing "normal" reflectivity minus any tuning noise. Linearly tuned seismic impedance therefore, is not representative of a real earth response, but is manufactured from a combination of the composite amplitude from interference, and to a lesser extent, the background amplitude that is noise free. Background reflectivity of a thin bed is a key factor in determining the

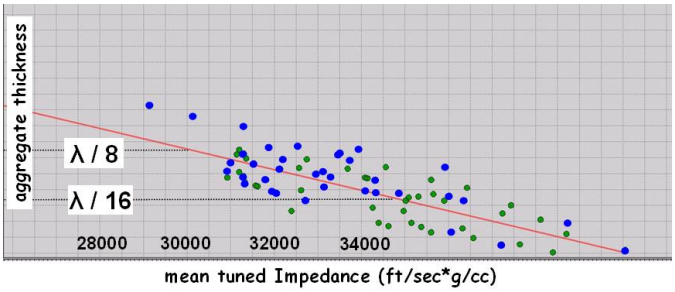

Fig. 10. The identical tuning model illustrated in figure 6 with estimated sand thickness (blue points) predicted from blind wells and "phantom" sands. Overall, the match is satisfactory relative to the prediction curve.

linearity limit that defines the *dynamic tuning range* as a function of reflectivity (equivalent to impedance), and measures the magnitude of gradient or slope characteristic of the tuning curve function. The dynamic tuning range ultimately defines the functionality of the amplitude tuning method, thus emphasizing the importance of the background reflectivity. This is illustrated analytically below by comparing tuning curves from a series of different tuning wedge models (figure 11) with varying degrees of background reflectivity. The series of tuning wedge models were created using a zero-phase 25 Hz Ricker wavelet with a vertical seismic sample rate of 2ms. Input rock property parameters for each tuning wedge model are listed in table 1 below. Tuning polarity is negative-positive (trough-peak), identical to our tuning wedge model discussed earlier, where a trough and peak represent a decrease and increase in impedance, respectively.

The various models are shown in Figure 11, and represent low velocity brine saturated porous sands encased in a high velocity non-porous shale. P-wave velocities and densities are proportionally increased to higher values with each progressive layer; the surrounding shales were assigned a constant p-wave velocity and density.

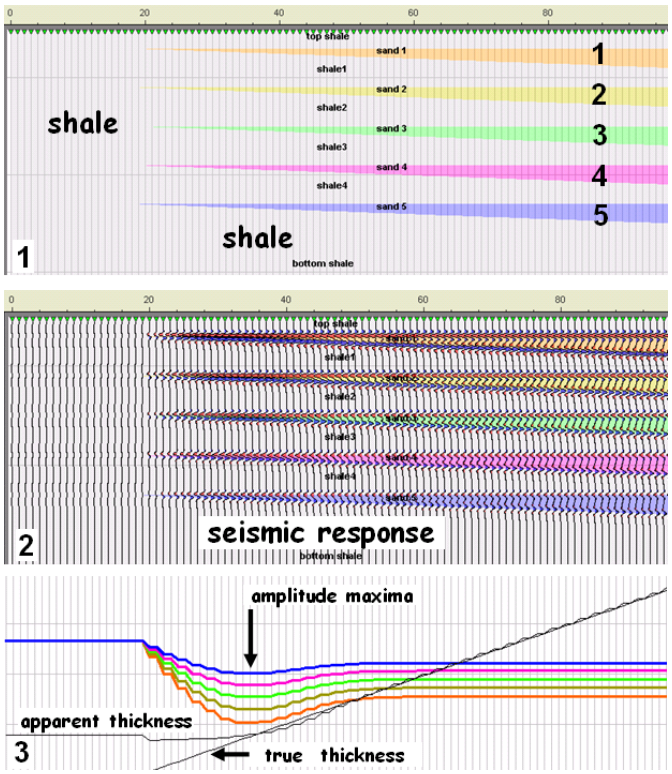

Fig. 11. Various tuning wedge models characteristic of input rock properties defined in table 1, and the relative seismic response to those properties (panel 2). The tuning curves are shown in panel 3. Notice the difference in gradients (or slopes) where the tuning curves are linear. This defines the background reflectivity minus any tuning. The same curves are depicted in figure 12 with rotated axes.

Wedge layer 1 (panel 1) is characteristic of the lowest p-wave velocity and density relative to the high velocity encasing shale, and therefore exhibits the highest magnitude of reflectivity which corresponds to the brightest amplitude response of all the layers (panel 2). The resultant tuning curve is shown in panel 3, and is color coded appropriately according to wedge layer, as are all amplitude maxima. Notice layer 1 (orange curve) is characteristic of the largest maximum amplitude due to its high magnitude of reflectivity. The remaining layers show a proportionally similar decrease in reflectivity and amplitude response as the rock properties of the layers increasingly approach the p-wave and density values characteristic of the encasing shale. Layer 5 shows the least reflectivity, which is apparent of the corresponding tuning curve (blue).

The background reflectivity of the five wedge models is defined by the tuning curves in panel 3, which are displayed using identical scales. The tuning curves are responding to various degrees of reflectivity characteristic of the impedance contrasts between the sands and shale defined in table 1. The relative differences in gradients (or slope) are observed at the linear potions of the curves experiencing tuning. The gradients tend to show a decrease in magnitude by a factor relative to

Wedge Layer	Color	velocity (m/sec)	Density (g/cc)	Impedance (m/sec*g/cc)
1	orange	3050	2.25	6863
2	yellow	3280	2.30	7544
3	green	3505	2.35	8237
4	purple	3735	2.40	8964
5	blue	3960	2.45	9702
encasing shale	cyan	4270	2.72	11614

Table 1. The rock properties characteristic of the tuning wedge models in figure 11.

the reflectivity inherent to the layer, which is referred to a the *background reflectivity*. Hence, larger reflectivity contrasts result in steeper gradients and a wider breadth of dynamic tuning. It is therefore apparent from the wedge models that the linearity portion of the tuning curve is not only a function of aggregate thickness and tuning amplitude, but the result of background reflectivity as well, which is proportional to the gradient r_t / d defined in equation 6.

This is shown more clearly in figure 12 (panel 1) where the tuning curve axes have now been rotated, and plotted in a form according to the gradient defined above, where r_t is equivalent to tuned seismic impedance. The color scheme representing the wedge layers defined in figure 11 has not changed. Again, the orange curve (wedge layer 1) shows the greatest magnitude of reflectivity, and therefore the steepest gradient relative to the other layers and shows the largest dynamic range or breadth of possible tuning reflectivity or impedance. The opposite is true of the blue curve with the least breadth of background reflectivity, characteristic of a minimal degree of gradient.

This may tell us that the background reflectivity, that is free of any tuning (noise), may act as a diagnostic indicator in defining the functionality of any tuning study prior to its onset and what the expectations may be. Conceptually for example, we would expect shallower, relatively younger formations to be more characteristic of wedge layers 1 and 2 due to higher a magnitude background reflectivity. Significantly shallower rocks would be characteristic of lower effective pressures allowing for additional open cracks and greater porosities, and hence slower formation velocities. Thus, the larger background reflectivity at shallower depths would increase the dynamic range of the tuning, and potentially the functionality of the method. The opposite would be true for deeper and older rocks where greater effective pressures have closed cracks and decreased porosity; rocks would be characteristic of higher velocities and potentially less reflectivity relative to the non-porous encasing shale resulting in a minimal dynamic rang of tuning.

Changes in the type and degree of fluid saturation can also affect background reflectivity considerably. The tuning wedge models defined in figure 11 were initially created 100% brine saturated, which was then replaced with 70% gas saturation and 30% brine; the effects of which are apparent in figure 12 (panel 2). The modeled sands have now become more compressible with the addition of gas. Lower p-wave velocity, and to some extent density, have increased reflectivity as impedance contrasts between the sands and shale have increased. The tuning curves show (Figure 12, panel 2) that background reflectivity for all layers has increased to some degree in magnitude, which is also apparent in the increase in amplitude maxima. This has resulted in an increase in the dynamic range of tuning reflectivity characteristic of the tuning curves, which is especially true for wedge layers 1 and 2 which show are sharp increase in gradient. The change in gradient magnitude, as function of gas saturation, may be diagnostic of fluid type.

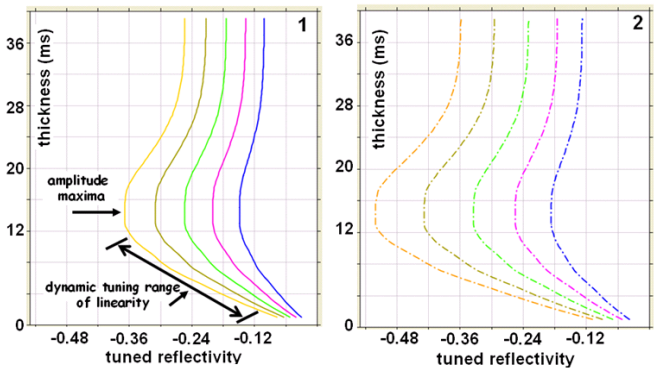

Fig. 12. Tuning curves representative of the various tuning wedge models shown in figure 11. Tuned reflectivity is equivalent to tuned seismic impedance. Notice the increasing range or breadth of the linearity as the gradient (equation 6) changes. Panel 2 shows the seismic amplitude response with 70% gas saturation. The changes in the amplitude response have resulted in steeper gradients for all curves representative of a fluid indicator.

Conclusions

Tuning amplitude, representative of tuned seismic impedance, has successfully predicted aggregate sand thickness characteristic of the deep gas Tuscaloosa trend where reservoir sands are typically below ¼ tuning thickness and are not resolvable by the seismic data. Aggregate sand thickness has been predicted at 37 blind well locations, including 13 "phantom" sand locations which represent sands predicted from vertically dissimilar stratigraphic formations, not related to sand X. Thus, if seismic frequency and velocity remain relatively consistent, the tuning model (calibrated to sand X) conceivably could be used for sand thickness prediction of additional stacked sands.

The majority of the blue dots depicted in figure 10 represent predicted thickness points which satisfactorily plot near the prediction curve. There are some outliers that plot away from the curve for reasons most likely attributed to first order effects caused by noisy seismic data due to amplitude attenuation at such great depths, and possible second order effects attributed to frequency and p-wave velocity inconsistencies as the method is parameterized according to these variables. Predicted aggregate thickness measurements have been successfully used in the estimation of volumetrics and hence, hydrocarbon reserves for appropriate short-listing of the prospect inventory. Overall, the method was a success and aggregate sand prediction from tuning amplitude was accurate. Moreover, the ability to discern reservoir thickness changes at depths approaching 7000 meters, with seismic data inundated with noise, is notable.

References

Widess, M. B., 1973, How thin is a thin bed?: Geophysics, v. 38, no. 6, p. 1176-1180.

Soroka, W.L., and M.L. Shoemaker, 2003, Impedance inversion in a structurally complex carbonate environment: 73rd Annual International Meeting, SEG, Expanded Abstracts, p. 398-401.

Shoemaker, M.L., W.A., Hill, P.T., Trumbly, 2006, Implications of wavelet analysis to reservoir quality and reserve estimation: A systematic approach to wavelet estimation with an example case study from the deep Tuscaloosa Trend, Pointe Coupe Parish, Louisiana, USA: 76th Annual International Meeting, SEG, Expanded Abstracts, p. 1103-1107.

Jankins, F. A., and White, H. E., 1957, Fundamentals of optics: New York, McGraw Hill Publishing Co.

Kallweit, R. S., and Wood, L. C., 1982, The limits of resolution of zero-phase wavelets: Geophysics, 47, p. 1035-1046.

De Voogd, N., and Den Rooijen, H., 1983, Thin layer response and spectral bandwidth: Geophysics, 48, p. 12-18.

Okaya, D., A., 1995, Spectral properties of the earth's contribution to seismic resolution: Geophysics, 60, p. 241-251.

Chungt, H., and Lawton, D., C., 1995, Amplitude responses of thin beds: Sinusoidal approximation versus Ricker Approximation: Geophysics, 60, p. 223-230.

Hill, J. H., 2005, Inversion-based thickness determination: The Leading Edge, p. 477-480.